10B.3 **Real time identification and filtering of ground clutter**

S.M. Ellis*, J.C. Hubbert, M. Dixon and G. Meymaris
National Center for Atmospheric Research, Boulder CO

1. INTRODUCTION

The identification and mitigation of anomalous propagation (AP) and normal propagation (NP) clutter is an ongoing problem in radar meteorology. Scatter from ground clutter targets routinely contaminates radar data and masks weather returns causing poor data quality. The problem is typically mitigated by applying a clutter filter to all radar data but this also biases weather data with near zero radial velocity. Modern radar processors make possible the real time identification and elimination of AP clutter. To this end, a fuzzy logic algorithm, referred to as Clutter Mitigation Decision (CMD), has been developed to distinguish between clutter echoes and precipitation echoes. Subsequently a clutter filter is applied to those radar resolution volumes where clutter is present and the radar moments computed from this selectively clutter filtered data. In this way zero velocity weather echoes are preserved while clutter echoes are mitigated. Since the radar moments are recalculated from clutter filtered echoes, the underlying weather echo signatures are revealed thereby significantly increasing the visibility of weather echo. Single polarization and dual-polarization versions of CMD have been developed and tested and are described in detail in Hubbert et al. (2006) and Hubbert et al. (2009a, 2009b). The single polarimetric version of CMD is currently scheduled to be deployed on the National Weather Service operational radar network, Weather Surveillance Radar 1988 Doppler (WSR-88D) beginning in the spring of 2009.

Two external factors that potentially impact the performance of the CMD algorithms are mixed weather and clutter conditions, and ground clutter echoes from trees that are in motion due to the wind in heavily forested regions. The goal of this study is to determine the impact of these factors on the CMD algorithms.

Weather echoes can be biased in the presence of ground clutter echoes even if the clutter is weaker than the weather echoes, in other words negative Clutter to Signal Ratios (CSR; in dB). Friedrich et al. (2008) showed that dual-polarimetric variables are biased with CSR values as low as -10 dB. Therefore it is important to determine how the CMD algorithm performs as a function of CSR. In this study we investigate the characteristics of the different CMD inputs, as well as the overall performance of CMD as a function of CSR.

The Clutter Phase Alignment (CPA) is a valuable input into CMD. It is a measure of temporal phase fluctuations of echoes over typical data collection times for a single radar resolution volume. CPA is defined as the magnitude of the vector sum of the individual time series members, x_i divided by the sum of the magnitudes of the x_i:

$$CPA = \left| \sum_{i=1}^{N} x_i \right| / \left[\sum_{i=1}^{N} |x_i| \right],$$

where N is the number of samples in the radar resolution volume. Thus, CPA ranges from 0 to 1 with 1 indicating a very high probability of clutter. Intuitively, CPA is a good indicator of clutter since by definition it is a metric of the primary characteristic of a stationary ground clutter target, i.e., low variability of backscatter phase. CPA will be a maximum for targets with 0 m s^{-1} radial velocity and narrow spectrum width (Hubbert et al. 2009a) and will decrease with increasing spectrum width. Therefore, it is necessary to determine the impact on CPA, and ultimately CMD performance, of trees and vegetation in motion due to wind, which may increase spectrum width compared to stationary clutter. In this study we examine CPA values in echoes from the heavily forested mountains of Southern Taiwan at various wind speeds.

2. CMD IN MIXED WEATHER AND CLUTTER

The inputs for the single and dual polarization CMD algorithms are listed in Table 1. The inputs except CPA are computed over a specified number of range gates along a single azimuth. Details of the input variable calculations can be found in Hubbert et al. (2006), and Hubbert et al. (2009b). Radar data from NCAR's S-band dual polarimetric radar (S-Pol) were collected in conditions of mixed weather and clutter. The GMAP spectral domain clutter filter was run on

*Corresponding author address: Scott Ellis, NCAR P.O. Box 3000, Boulder, CO 80307-3000, sellis@ucar.edu

the data throughout the domain. The GMAP outputs the power of the clutter removed, so in the absence of near zero velocity weather this information can be used to compute the Clutter to Signal Ratio. The CMD algorithms were then run and the individual inputs and overall results analyzed as a function of the computed CSR. Pure clutter and pure weather data were also available from S-Pol for comparison.

CMD Input Variable	Single-Pol	Dual-Pol
Clutter Phase Alignment (CPA)	✓	✓
SPIN	✓	✓
Texture of Reflectivity (TDBZ)	✓	✓
Standard Deviation of Z_{DR} (SDZDR)		✓
Standard Deviation of Φ_{DP} (SDPHI)		✓

Table 1. Listing of CMD input variables, indicating which are used for the single and dual polarization algorithms.

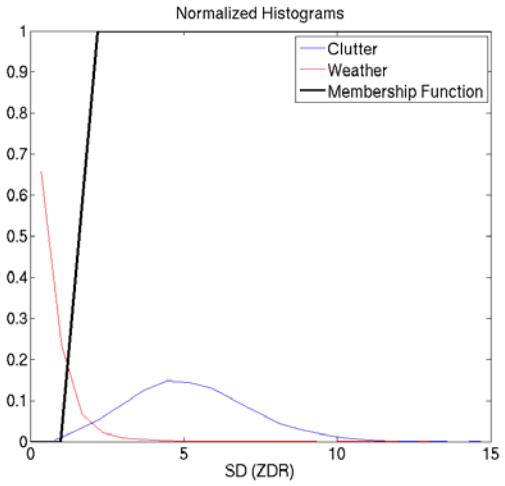

Figure 1. Normalized histograms of SDZDR for pure clutter and pure weather. The black line indicates the SDZDR membership function in CMD. The y-axis is the normalized frequency of occurrence.

Figure 1 shows normalized histograms of the standard deviation of Z_{DR} (SDZDR) for pure clutter (blue) and pure weather (red). The thick black line indicates the membership function for SDZDR used in the CMD algorithm. The membership function is designed so that 1 strongly indicates clutter and 0 strongly indicates no clutter with a smooth transition between. It can be seen that the separation of pure weather and pure clutter for this variable is quite good, with only a small overlapping area near values of 2.5.

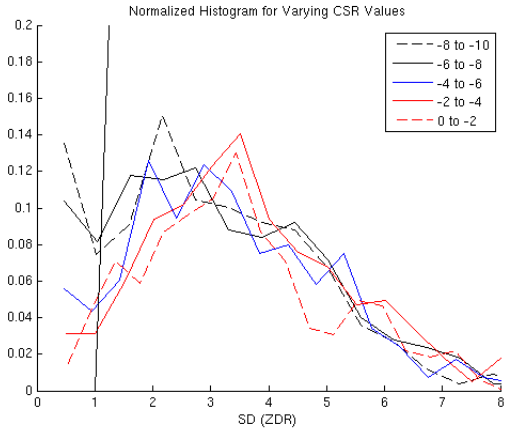

Figure 2. Normalized histograms of SDZDR for various ranges of CSR values. The black line indicates the SDZDR membership function CMD. The y-axis is the normalized frequency of occurrence.

Figure 2 shows normalized histograms of SDZDR at different ranges of CSR values (dB). The SDZDR membership function is again plotted in black. The histogram for CSR between 0 and -2 dB is similar to the pure clutter case shown in Figure 1. However as the CSR decreases the histograms become bimodal with a maximum at very low SDZDR values. Surprisingly the two modes of the lower CSR histograms resemble the pure clutter and pure weather distributions. At a CSR range between -8 and -10 dB roughly half of the range gates have low enough SDZDR that they are not classified as clutter by this input.

Figure 3 is similar to Figure 1 but for the standard deviation of Φ_{DP} (SDPHI). It can be seen that the separation of pure weather and pure clutter in the case of SDPHI is even better than that of SDZDR, with the clutter and weather peaks being further spaced and there is less overlap between the categories.

Figure 4 is similar to Figure 2 but for the SDPHI. As for SDZDR the 0 to -2 dB CSR range histogram is similar to the pure clutter shown in Figure 3 and the histograms become bimodal with decreasing CSR values. Again one mode resembles the pure clutter and the other mode resembles the pure weather.

Figures 5 and 6 present similar plots as Figures 1 and 2 except they are for the texture of reflectivity (TDBZ). It can be seen in Figure 5 that

the separation of the pure weather and pure clutter for TDBZ is good but, not surprisingly, not quite as good as the dual polarimetric derived inputs of SDZDR and SDPHI. The normalized histograms of TDBZ in Figure 6 have different characteristics from the SDZDR and SDPHI as the CSR decreases. In this case there are not noticeable bimodal distributions at lower CSR values, but instead the histograms increasingly resemble the pure weather as CSR decreases.

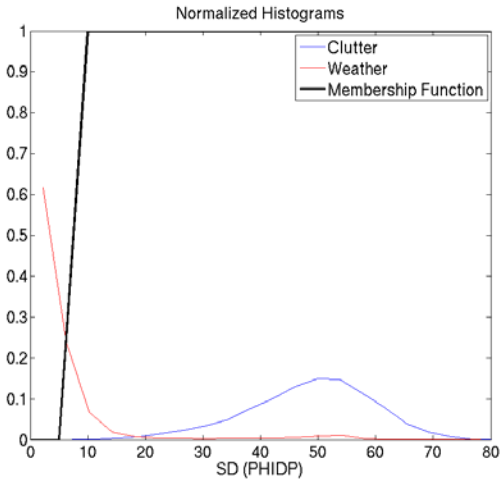

Figure 3. Similar to Figure 1 for SDPHI

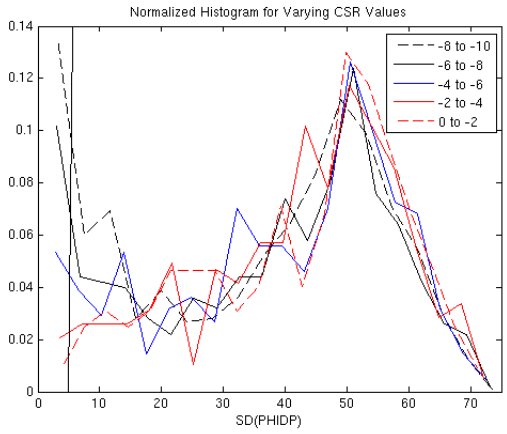

Figure 4. Similar to Figure 2 for SDPHI

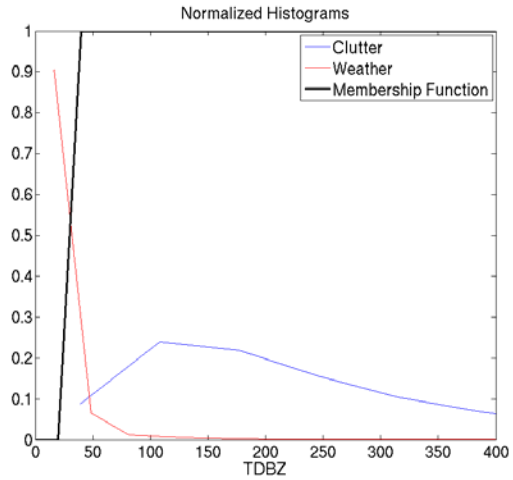

Figure 5. Similar to Figure 1 for TDBZ

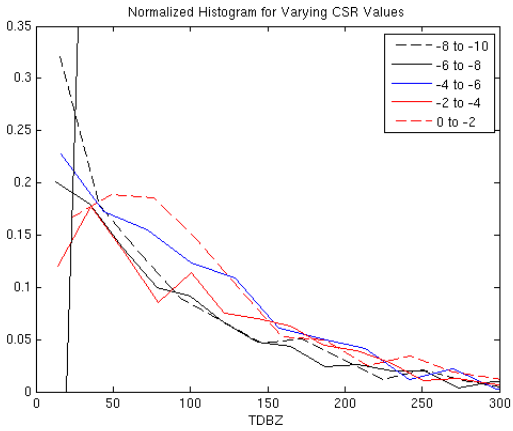

Figure 6. Similar to Figure 2 for TDBZ

Figure 7 shows histograms in pure weather and pure clutter for the SPIN input variable. The curves are not as smooth owing to the quantized nature of the SPIN variable. The separation of pure clutter and weather using SPIN is seen to be quite good with very little overlap. Figure 8 shows the normalized histograms for various CSR values of the SPIN input variable. As CSR decreases the SPIN variable displays a bimodal distribution, until the CSR range is -8 to -10 dB. At this range the SPIN variable mostly resembles the pure weather values with the majority of the range gates indicated as weather.

Figure 9 shows the normalized histograms at different CSR ranges for the CPA variable. The distribution becomes bimodal with decreasing CSR. Notice that CPA is able to detect more range gates with clutter at smaller CSR values than for SPIN or TDBZ.

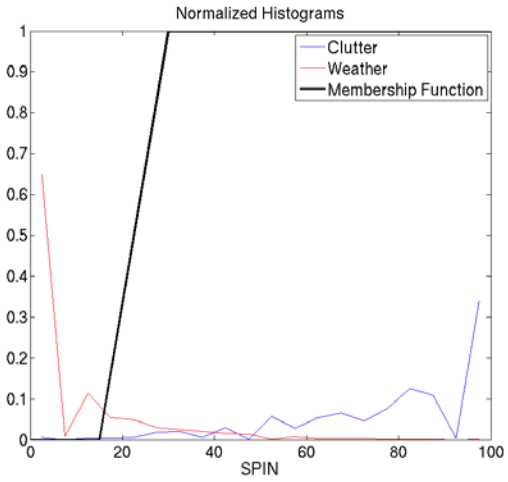

Figure 7. Similar to Figure 1 for SPIN

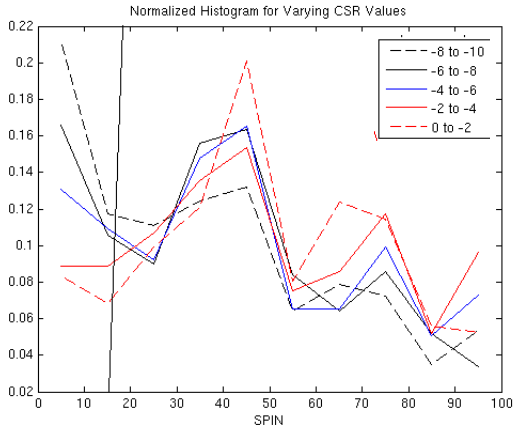

Figure 8. Similar to Figure 2 for SPIN

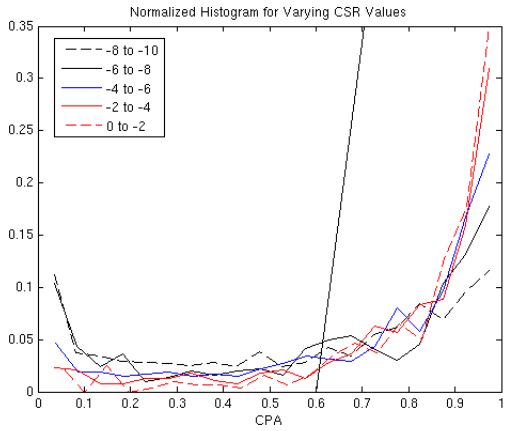

Figure 9. Similar to Figure 2 for CPA

From Figures 1 through 9 it can be seen that the separation of pure weather and pure clutter and also the detection of the presence of ground clutter at low CSR values is better for the dual polarimetric variables and CPA than for the single polarization inputs of TDBZ and SPIN. Therefore it would be expected that the addition of the dual polarimetric variables to the single polarization CMD algorithm would improve the performance, particularly at lower CSR values. This is illustrated in Figure 10, which shows the fraction of range gates identified by CMD and subsequently filtered (solid lines) and the fraction of unfiltered (dashed lines) range gates as a function of CSR for the single polarization algorithm (thin lines) and the dual polarimetric algorithm (thick lines). Range gates with SNR less than 10 dB are excluded. Note that the curves for the fraction of filtered and unfiltered are complementary, i.e. one minus the fraction filtered line value gives the fraction unfiltered line value. The improved performance with the addition of SDZDR and SDPHI (with appropriate modification of the weights) can be seen by the dual polarimetric curves lying to the left of the single polarization curves. The 50% detection level for the single polarization algorithm is close to -10 dB CSR, while the dual polarization is closer to -13 dB.

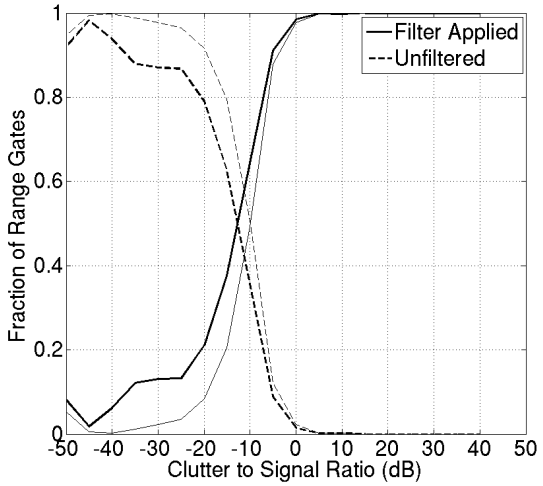

Figure 10. Comparison of the fraction of range gates identified by CMD for filtering between the dual pol (thick lines) and single pol (thin lines) algorithms. The solid lines indicate the fraction of gates identified for filtering and the dashed lines indicate the fraction of unfiltered gates.

3. CPA IN FORESTED REGIONS

In order to determine the impact of wind blown trees on the CPA input variable S-Pol data were collected on three clear days in Southern Taiwan with varying wind speeds as determined

by surface stations. This clutter data originated in the heavily Central Mountain Range and were collected on June 6, June 13 and June 17, 2008 during the Terrain-influenced Monsoon Rainfall Experiment (TiMREX) field experiment. The wind speeds on those days were 0 to 5 MPH, 5 to 10 MPH and 10 to 15 MPH, respectively. Histograms of the three data sets are shown in Figures 11, 12 and 13. Range gates identified to contain clutter on the calm day (June 6) were used in the analysis of all three days. Note that S-Pol used indexed beams during TiMREX, so the results from all three days contain data from the same range bins in the same locations. It can be seen that the distributions of CPA did not vary noticeably at the differing wind speeds. In fact the mean CPA values were nearly identical: 0.89 (0-5 MPH wind), 0.88 (5-10 MPH wind) and 0.89 (10-15 MPH wind). One explanation is that the clutter reflectivity was dominated by the larger more stable portions of the tree such as the trunks and thick branches, so that the power returned by the smaller, moving leaves and branches was overwhelmed.

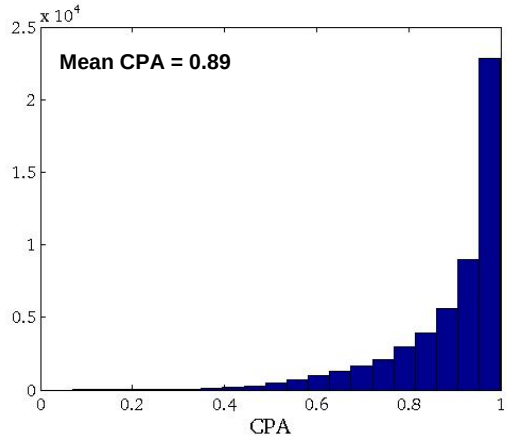

Figure 11. Histogram of CPA in forested clutter region on June 6 with wind speeds from 0 to 5 MPH.

4. CONCLUSIONS

The performance of the single and dual polarization CMD algorithms was evaluated as a function of CSR. The inputs were all found to have very good detection of clutter at negative values of CSR. The SDZDR, SDPHI and CPA had superior detection at low CSR to SPIN and TDBZ. The performance of the complete CMD algorithms showed that the single polarization algorithm had a 50% detection rate at a CSR of about -10 dB. It was also shown that the dual polarization performance was improved with the 50% detection rate closer to -13 dB.

The CPA was shown to be consistent in heavily forested regions independent of wind speed. This is important given the fact that the CMD algorithm will be deployed across the United States in different clutter environments.

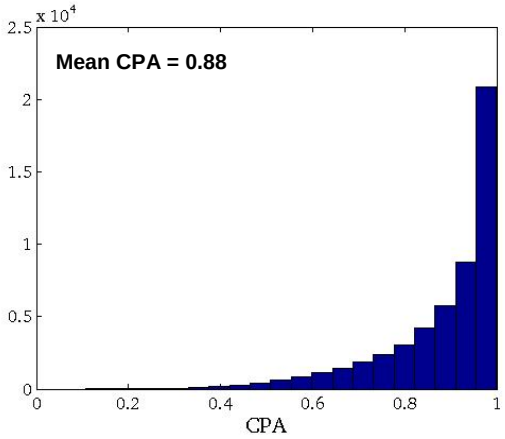

Figure 12. Histogram of CPA in forested clutter region on June 13 with wind speeds from 5 to 10 MPH.

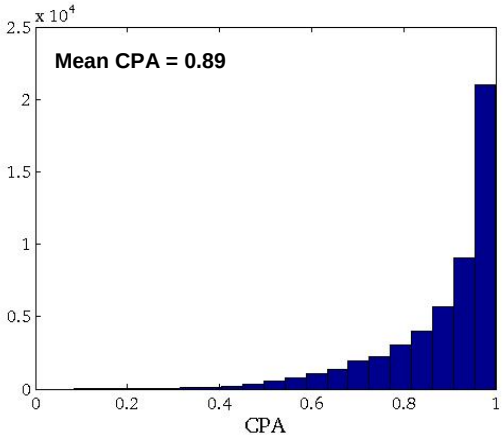

Figure 13. Histogram of CPA in forested clutter region on June 17 with wind speeds from 10 to 15 MPH.

References:

Friedrich K, Germann U, Tabary P (2008) Influence of Ground Clutter Contamination on Polarimetric Radar Parameters. *Journal of Atmospheric and Oceanic Technology*: In Press

Hubbert, J. C., M. Dixon, and S. M. Ellis, 2008. Enhancements in Clutter/ Precipitation Discrimination for the WSR-88D. *Preprints, European Radar Conf, ERAD*, Helsinki Finland, July 2008.

Hubbert, J. C., M. Dixon,, S. M. Ellis, and G. Meymaris 2009a. Weather Radar Ground Clutter, Part I: Identification, Modeling and Simulation. *Journal of Atmospheric and Oceanic Technology*: Accepted

Hubbert, J. C., M. Dixon, and S. M. Ellis, 2009b. Weather Radar Ground Clutter, Part II: Real Time Identification and Filtering. *Journal of Atmospheric and Oceanic Technology*: Accepted